In Silico Investigation of Cardiac Arrhythmia Susceptibility in Long QT Phenotype

Anthony Owusu-Mensah
Biomedical Engineering
Old Dominion University (ODU)
Norfolk, USA
email: aowus003@odu.edu

Vicky Lam
Biomedical Engineering
Old Dominion University (ODU)
Norfolk, USA
email: vlam009@odu.edu

Bright Tsevi
Department of Engineering
Norfolk State University (NSU)
Norfolk, USA
email: b.tsevi@spartans.nsu.edu

Michel Audette
Computational Modeling and Simulation Engineering
Old Dominion University (ODU)
Norfolk, USA
email: maudette@odu.edu

Makarand Deo
Department of Engineering
Norfolk State University (NSU)
Norfolk, USA
email: mdeo@nsu.edu

***Abstract*— Long QT Syndrome (LQTS) is associated with cardiac arrhythmia and sudden cardiac death. The Long QT Type 2 (LQT2) phenotype, which accounts for 35–40 % of all LQTS patients, is caused by mutations in HERG gene. The mechanisms of arrhythmia in presence of LQT2 conditions are not fully understood. We utilized anatomically and electrophysiologically realistic numerical simulations to elucidate the mechanisms of arrhythmia initiation in presence of blockade in rapid component of delayed rectifier potassium current, I_{Kr}. We utilized a 3D finite element model of rabbit ventricles integrated with His-purkinje network to simulate whole heart response to LQT2 conditions. We observed that the loss of I_{Kr} function produced more severe phenotype in cardiac Purkinje cells than that in ventricular myocytes. Our simulations also revealed that arrhythmia susceptibility is increased when there is a loss of I_{Kr} functionality. Our multi-scale computer modeling results provide useful insights into the potential mechanisms of arrhythmia in LQT2 conditions.**

Keywords-Long QT Syndrome(LQTS); Cardiac modeling; Arrhythmia; Reentry;Purkinje fibers.

I. INTRODUCTION

The Long QT syndrome (LQTS) is an acquired or congenital cardiac electrical disorder characterized by the prolongation of the QT interval on an ECG, which is associated with life-threatening ventricular arrhythmias and sudden cardiac death [1]–[3]. Gene mutations in KCNQ1 (the gene that encodes slow delayed rectifier potassium current, IKs), HERG (the gene that encodes rapid delayed rectifier potassium current, I_{Kr}), and SCN5A (the gene that encodes fast inward sodium current, I_{Na}) are responsible for LQT1, LQT2, and LQT3 respectively, which account for 95% of the congenital LQTS in patients [3]–[5]. In LQT2, mutations in HERG cause partial or complete blockade of I_{Kr} which delays the repolarization process causing action potential (AP) prolongation and subsequent prolonged QT interval in ECG. A myriad of I_{Kr}-blocking drugs, such as E-4031 (benzenesulfonamide), dofetilide or D-sotalol, may also lead to drug-induced LQTS [2]. Arrhythmia occurrence has been well documented in LQT2 patients, but exact mechanisms are still poorly understood.

Numerical biophysical models with high fidelity can offer the missing mechanistic link between experimental or clinical findings and their therapeutic implications. Fortunately, very advanced biophysical computer models, numerical techniques and computing facilities are available today to conduct realistic “numerical experiments”. We have used detailed computer modeling to study the functional effects of various cardiac mutations [6]–[8] as well as to investigate complex arrhythmia mechanisms [9][10]. Iyer et al. used computer models of Purkinje Cell (PC) and Ventricular Myocyte (VM) to study alterations in channel functions in different LQT phenotypes and concluded that the His-Purkinje system (PS) may represent an important therapeutic target for heritable channelopathies [11].

Seemann et al. [12] used a heterogeneous and anisotropic three-dimensional computational model of the human ventricles to study LQT1, LQT2, and LQT3. Recently, patient-specific numerical models of LQTS using human induced pluripotent stem cell derived cardiomyocytes

 ISBN: 978-1-61208-898-3

(hiPSC-CMs) have been used to investigate the loss of repolarizing currents on AP abnormalities [3][13][14]. The high incidence of LQT2 compared to other LQTS types except for LQT1 [15] and the significant consideration of the blockade of HERG channels in the developmental process for new drugs makes it more imperative to have a complete understanding of the mechanisms of LQT2 [16].

In this paper, we present a multiscale computer modeling approach to investigate the effects of complete or partial I_{Kr} blockade at single cell and 3D ventricular anatomy levels in rabbit heart. The effects of I_{Kr} block on AP morphology in two cell types: ventricular myocytes (VM) and cardiac Purkinje cells (PCs), and implications on reentry initiation in ventricles were studied systematically.

This paper is composed of four main sections. In section 1, which is the introduction, gives an overview of LQTS. A literature review on how LQTS has been studied both in simulation and experimentation. It then follows up with a justification for studying LQT2 syndrome and the approach we used for the studies. Section 2 describes how we performed single cell biophysical and 3D anatomical simulations respectively. We further explained how reentry was initiated in the 3D anatomical model. The results section follows section 2, and it gives an account of the observations from our simulations. In section 3(discussion), we discussed our results and compared them to our findings in literature. The last section(conclusion) provides a summary of our work and the outcomes likely to result from it.

II. METHODS

A. Single cell Biophysical Simulations

Single cell AP simulations were performed using rabbit VM biophysical model by Mahajan et al. [17] and rabbit PC model by Aslanidi et al. [18]. Both models were paced at 500 ms basic cycle length (BCL) for 50 sec to attain steady state before they were used in simulations. I_{Kr} was blocked from 0% (Control) to 100% (complete blockade) by applying corresponding scaling to the maximum conductance of I_{Kr} and its effect on AP durations at 50% and 90% repolarization (APD_{50} and APD_{90}, respectively) were studied in both tissue types.

B. 3D Anatomical Simulations

The 3D simulations were performed in a rabbit ventricular anatomical model. The model consists of a finite element tetrahedral mesh, based on the San Diego rabbit heart [19], consisting of 547,680 myocardial nodes (862,515 nodes including surrounding bath and cavities), with an average internodal spacing of 250 μm (see Figure 1). LV and RV stand for are left ventricle and right ventricle, respectively.

The PS comprised of a branching network of one-dimensional cubic Hermite elements. PS nodes were separated by discrete gap junctions that were modeled as fixed resistances. The purkinje-myocardial junctions (PMJs) were modeled as resistive junctions as described in [20]. The electrical activity in the tissue was modeled by bidomain

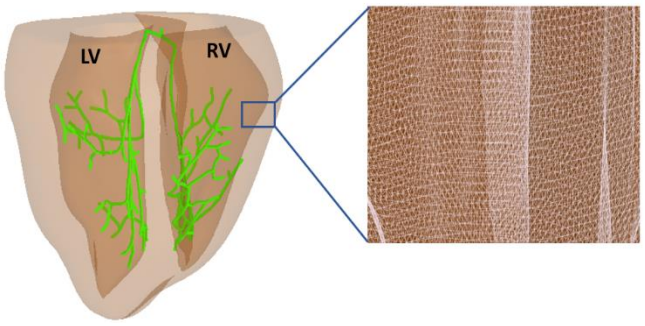

Figure 1. 3D computational mesh of rabbit ventricles integrated with PS (green color) used in our study. The inset shows the mesh discretization.

equations as described elsewhere [10][20]. The intracellular, Φ_i and extracellular, Φ_e potentials are related through the transmembrane current density, I_{m} by the equations:

$$\nabla.(\bar{\sigma}_{\mathrm{i}} + \bar{\sigma}_{\mathrm{e}})\nabla\Phi_{\mathrm{e}} = -\nabla.\bar{\sigma}_{\mathrm{i}}\nabla V_{\mathrm{m}} - I_{\mathrm{e}} \quad (1)$$

$$\nabla.\bar{\sigma}_{\mathrm{i}}\nabla V_{\mathrm{m}} = -\nabla.\bar{\sigma}_{\mathrm{i}}\nabla\Phi_{\mathrm{e}} + \beta I_{\mathrm{m}} \quad (2)$$

$$I_{\mathrm{m}} = C_{\mathrm{m}}\frac{\partial V_{\mathrm{m}}}{\partial t} + I_{\mathrm{ion}}(V_{\mathrm{m}}, \nu) - I_{\mathrm{trans}} \quad (3)$$

, where $\bar{\sigma}_{\mathrm{i}}$ and $\bar{\sigma}_{\mathrm{e}}$ are the intracellular and extracellular conductivity tensors respectively, β is the surface-to-volume ratio of the cardiac cells, I_{trans} is the transmembrane current density stimulus as delivered by the intracellular electrode, I_{e} is the extracellular stimulus current density, C_{m} is the membrane capacitance per unit area, V_{m} is the transmembrane voltage which is defined as $\Phi_i - \Phi_e$ and I_{ion} is the current density flowing through the membrane ionic channels which depends on the transmembrane voltage and several other variables ν [28].

The membrane biophysics of ventricular myocardium (V) was simulated by Mahajan et. al. model [17] whereas that of Purkinje network was simulated by Aslanidi et al. model [18].

To simulate sinus rhythm activity, stimulus was applied to the top nodes of His bundle with BCL of 500 ms for at least 5 sec before any simulation protocol was applied. To ascertain the cardiac activity in the presence of LQT2 phenotype, maximum conductance of I_{Kr} in both V and PS was reduced by a percentage (25% block, 50% block and 100% block). Pseudo ECGs were generated by extrapolating the extracellular potentials to approximate limb locations for leads I, II and III.

C. Reentry Induction Protocol

Reentry was simulated by S1-S2 protocol for Control and 100% I_{Kr} block in V and PS. The myocardial conductivity in the model was reduced by 50% to slow the conduction and accommodate reentry wavelength in the tissue. Both models were paced at His with BCL of 500 ms for 5 sec to simulate sinus rhythm (S1). Then an ectopic stimulus (S2 stimulus) was delivered to a quarter region of myocytes on the right ventricle. The S1-S2 duration was varied between 200-300ms

 ISBN: 978-1-61208-898-3

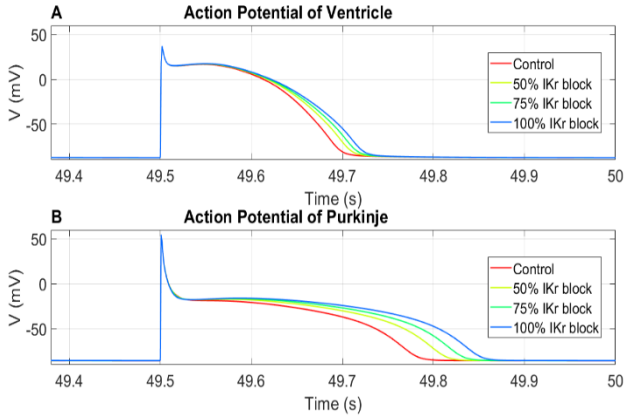

Figure 2. Action Potential Morphology. A: AP of ventricular myocyte for control, 50%, 75% and 100% I_{Kr} block. B: AP of the purkinje cell for control, 50%, 75% and 100% I_{Kr} block.

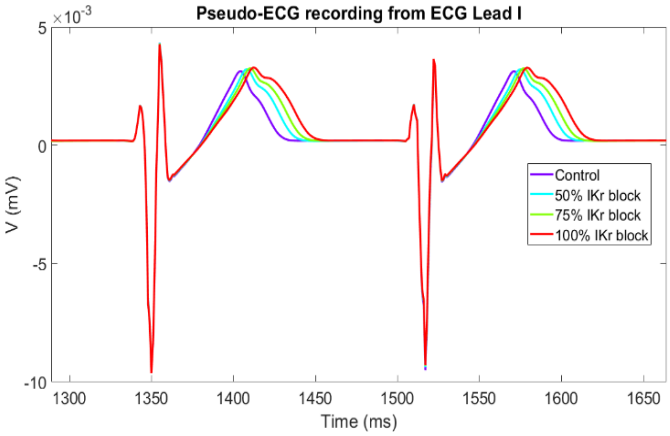

Figure 3. Lead I Pseudo ECG recording for Control,50%,75%, and 100% I_{Kr} block during sinus rhythm.

in the steps of 10 ms to determine a window of vulnerability to reentry initiation. The S1-S2 duration was varied in steps of 1-5ms within the window of vulnerability to allow fine-grain control of the timing at which reentry occurs. The reentrant activations were classified as tachycardia if they were sustained beyond 500 ms duration.

The 3D simulations were performed using Cardiac Arrhythmia Research Package (CARP), an in-silico cardiac simulator [21]. Single cell simulations were performed using bench utility in OpenCARP simulator [21]. All simulations were performed on High Performance
Computing (HPC) facilities of Old Dominion University (ODU) using 40 computing nodes and 2GB of physical memory per node.

III. RESULTS

A. *Ventricular myocyte and Purkinje cell action potential*

Figures 2A and B show the rabbit AP for both the VM and PC from the single cell simulations with varying I_{Kr} block ranging from 0% (Control)to 100% (complete blockade). Both the VM and PC APs exhibited the characteristic spike and dome morphology. In VM, the APD_{90} was prolonged by 13% as compared to the Control when I_{Kr} was completely blocked (192 ms in Control vs. 216 ms in 100% block). The effect of I_{Kr} block in PC was more severe in which the APD_{90} was prolonged by 26% when I_{Kr} was blocked completely

TABLE 1. APD_{90} AND PERCENTAGE PROLONGATION FOR 0%, 50%, 75% AND 100% I_{KR} BLOCK IN VENTRICULAR MYOCYTE (VM) AND PURKINJE CELL (PC) MODELS.

I_{Kr} block	**VM**		**PC**	
	APD_{90} (ms)	*% Prolongation*	*APD_{90} (ms)*	*% Prolongation*
0% (Control)	192	0	267	0
50%	203	6	299	12
75%	209	9	317	19
100%	216	13	336	26

(267 ms in Control vs. 336 ms in 100% block). Table 1 lists the percent prolongation in APD_{90} for various extents of I_{Kr} block in VM and PC models.

B. *Pseudo-ECG Recordings During Sinus Rythm*

Pseudo-ECGs for the primary three leads (I, II and III) were derived during sinus rhythm for Control and I_{Kr} block models. Figure 3 shows Lead I ECGs during sinus rhythm with aligned QRS for comparison. The QT prolongation was evident when I_{Kr} was blocked, and the extent of QT prolongation increased with the extent of I_{Kr} blockade.The QT duration measured was 94ms, 100 ms, 104 ms, and 114 ms for the control, 50% I_{Kr}, 75% I_{Kr} and 100% I_{Kr} block, respectively.

C. *Window of Vulnerability to Reentry*

Figure 4 summarizes the outcome of S1-S2 stimulation in Control and 100% I_{Kr} block models. If S2 stimulus occurred too soon, it was blocked by the refractory tissue (grey region). Whereas if S2 occurred too late, it was conducted by the entire ventricular tissue causing a premature excitation (blue region). When the S2 stimulus occurred when the tissue is partially excitable, more complex interactions were observed. In this case, the timing of the ectopic stimulus yielded the following consequences: 1) when myocytes in the vicinity of the stimulus were excitatory and right bundle branch (RBB) was excitatory, the ectopic stimulus induced activations in the right ventricle, which were picked up by the right distal purkinje fibers and conducted retrogradely through the PS.

The retrograde activations spread rapidly through the RBB exciting the left bundle branch (LBB) and the left ventricle, and 2) when myocytes in the vicinity of the stimulus were excitatory but the RBB was refractory, the right purkinje fibers blocked the activity from spreading through the RBB. The activations spread to the left ventricle via transseptal conduction instead. These two scenarios resulted in reentry and ventricular tachycardia (red region). It is also evident from the figure that the window of tachycardia occurrence is extended significantly when I_{Kr} is

 ISBN: 978-1-61208-898-3

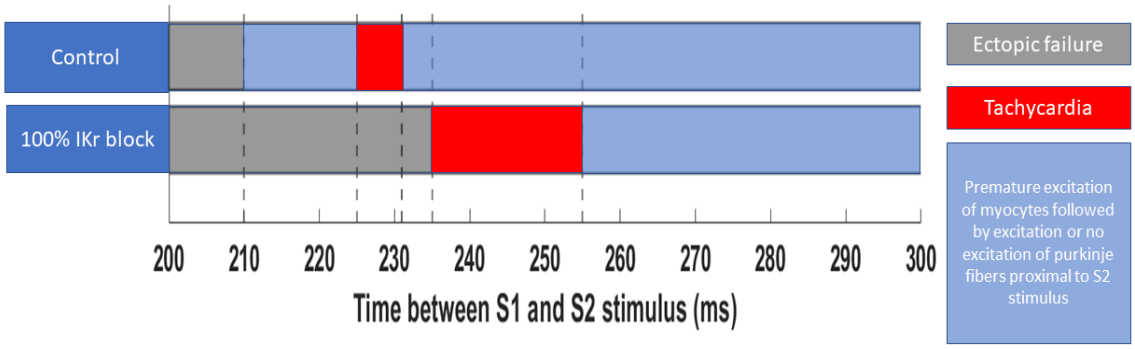

Figure 4. Conduction outcomes during reentry induction by S1-S2 window.

blocked. Thus, the ventricles are more susceptible to arrhythmia in presence of I_{Kr} block induced LQT2 phenotype.

D. Simulated Reentry Mechanism

Figure 5 shows a typical activation sequence in presence of 100% I_{Kr} block for a reentry duration that lasted at least 500 ms hence was referred to as tachycardia. The ectopic stimulus was delivered when the S1-S2 interval was 240 ms. When the ectopic stimulus was applied, the RV myocytes in the vicinity of the stimulus were excitatory while the RBB was refractory (Figure 5A). The ectopic stimulus induced activations in ventricles which were picked up by right distal PS network (see Figure 5A black arrow, V- P).

However, the excitation within the PS was blocked by the refractory RBB, thus preventing retrograde propagation towards the LBB. Excitations spread to the left ventricle via transseptal conduction (Figure 5A, white arrow). Due to the slowed conduction in the septum, the LBB recovers completely before the activation is picked up by the left distal PS network (Figure 5B). The activation excites the LBB which conducts retrogradely to the RBB, thus exciting the right PS and RV (Figure 5B, white arrow).

At 5500 ms, stimulus from the His bundle is blocked by both the RBB and LBB because both branches are refractory. Retrograde propagation from the LBB to RBB between 5500 and 5700 ms (Figure 5C) experiences a conduction block (CB) (Figure 5C, blue arrow). Excitation spreads to the right via transseptal conduction. Both bundle branches were now excitable as excitation reached the right (Figure 5D). Excitation from the ventricle (Figure 5D, black arrow, V-P) excites the RBB. Retrograde propagation (Figure 5D, yellow arrow, P-P) through the RBB reached the LBB, exciting it and the LV. Similar excitation pattern continued throughout the duration of tachycardia.

IV. DISCUSSION

In this study, we utilized single cell biophysical models of ventricular myocyte and Purkinje cell as well as 3D anatomical model of ventricles to investigate the susceptibility to arrhythmia in presence of HERG mutation leading to loss of I_{Kr} function. The main findings of our numerical study include: 1) loss of I_{Kr} function results in prominent QT prolongation in ECG, 2) the effects of I_{Kr} blockade on AP morphology are more severe in cardiac purkinje cells than that in ventricular myocytes, 3) the loss of I_{Kr} function increases the spatial dispersion of repolarization and refractoriness resulting into increased vulnerability to reentry and ventricular tachycardia, and 4) the His-Purkinje system plays an active role during maintenance of tachycardia.

A. AP Morphology in PC vs. VM

The characteristic spike and dome morphology was more prominent in the rabbit PC than in VM. Higher peak density of transient outward current (I_{to}) has been reported in rabbit PCs than ventricles [22] which produces the characteristic early repolarization in PCs. The inward rectifying potassium current (I_{K1}), which is responsible for keeping the cell at rest, is smaller in PC [22] than in ventricles. This results in a larger diastolic membrane resistance in PC allowing small charge displacements to cause significant changes in the membrane voltage [23]. The higher resistance accounts for the more substantial change in APD_{90} in PCs than VMs. I_{Kr} is the prominent repolarizing current in PCs. PCs also exhibit lower repolarization reserve than in VMs [27], hence the effects of I_{Kr} block on AP prolongation are more significant in PCs than VMs.

B. QT Prolongation in Pseudo-ECG

The limited availability of more definitive tests for LQTS makes ECG very important in its diagnosis [6]. Single-cell studies can only determine how much an APD is altered and cannot quantify the percentage QT prolongation. The widespread distribution of electrical pulses throughout the ventricles is mediated by the PS, and there is a significant change in the behavior of PS when it is coupled to a large mass of ventricular muscle [14] due to electrotonic loading. Our 3D model comprised of an integrated His-PS network which is capable of reproducing myocardial loading effects. Our model was able to successfully reproduce the prolonged QT interval and prominent notching of the T in ECGs corresponding to the loss of I_{Kr} as reported previously [6].

C. Arrhythmia in LQTS

Repolarization in cardiomyocytes depends on a delicate balance between various ionic currents. Abnormal repolarization of the AP provides a substrate for life-threatening cardiac arrhythmias. Early afterdepolarizations

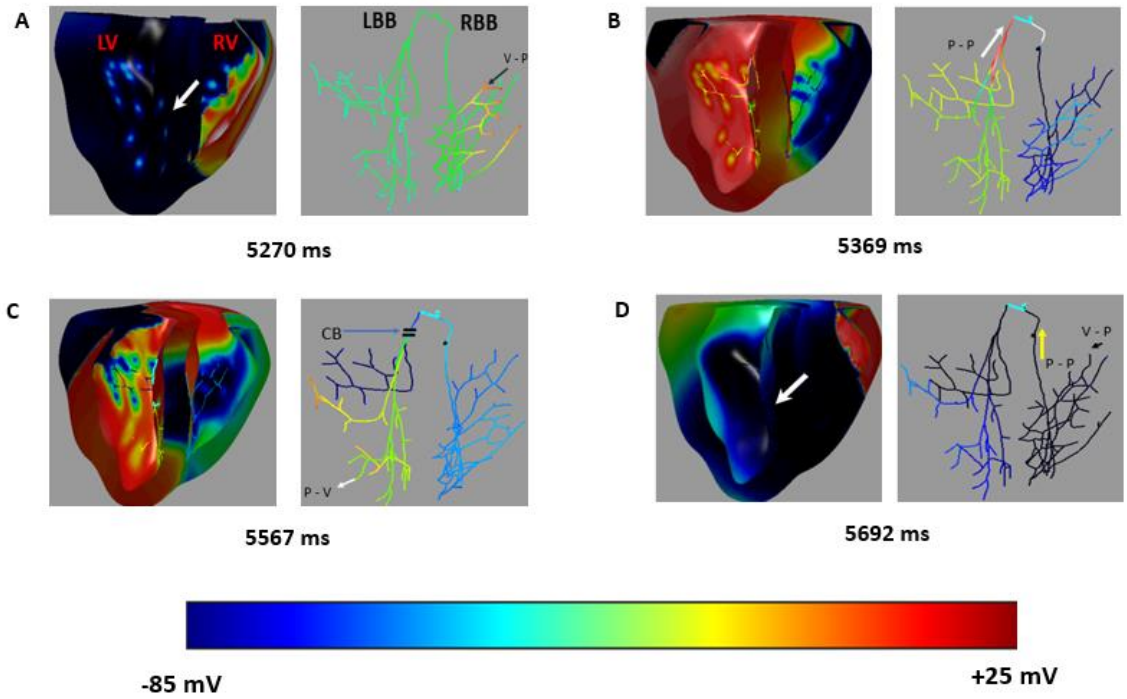

Figure 5. Reentry activations in the 3D ventricular model induced by an ectopic stimulus 270 ms post His-bundle activation. V-P: ventricular myocardium to Purkinje propagation; P-V: Purkinje to ventricular myocardium propagation; P-P: propagation within the Purkinje system; CB: conduction block.

(EADs), which are abnormal membrane depolarizations during the plateau or the repolarization phase of an AP, are thought to be responsible for arrhythmia initiation in LQTS. EADs increase substrate vulnerability (by increasing APD dispersion) and promote triggers for reentry formation [19]. In vivo monophasic AP recordings from the LV endocardium of rabbits induced with polymorphic ventricular tachycardia was preceded by deflections consistent with EADs in the monophasic APs [24]. The mutations in the HERG channel can prolong APD sufficient to generate EADs which may trigger life-threatening arrhythmias [25]. Electrophysiological studies of transgenic LQT1 and LQT2 rabbits reported prolonged APD and QT intervals; however atrioventricular (AV) blocks and polymorphic ventricular tachycardia were developed only in LQT2 rabbits [26].

In our study, we demonstrated tachycardia induction by applying a premature stimulus, which has a similar effect of EAD-induced tachycardia. More simulations are warranted to establish the mechanisms for increased susceptibility of the ventricular conduction system to trigger EAD-induced arrhythmia in LQT2 conditions.

V. CONCLUSION

We presented a multiscale numerical simulation study to investigate the arrhythmogenic effects of HERG channel block producing an LQT2 phenotype. Our model was able to reproduce clinically observed QT prolongation in ECG as a result of I_{Kr} block. Our study revealed that, a complete I_{Kr} blockade results into more severe phenotype in Purkinje cells than in ventricular myocytes. The window of susceptibility to reentry that degrades into tachycardia was significantly prolonged in presence of I_{Kr} block. Our simulation outcomes may provide vital insights into the mechanisms of arrhythmia susceptibility as observed in LQT2 patients.

ACKNOWLEDGMENT

The study was supported by the National Institutes of Health (NIH) award no. 1R15HL145530-01A1.

REFERENCES

[1] S. G. Priori, R. Bloise, and L. Crotti, “The long QT syndrome,” *Europace*, vol. 3, no. 1, pp. 16–27, 2001, doi: 10.1053/eupc.2000.0141.

[2] P. Kannankeril, D. M. Roden, and D. Darbar, “Drug-Induced Long QT Syndrome,” vol. 62, no. 4, pp. 760–781, 2010, doi: 10.1124/pr.110.003723.electrophysiologic.

[3] M. D. Lemoine *et al.*, “Human Induced Pluripotent Stem Cell-Derived Engineered Heart Tissue as a Sensitive Test System for QT Prolongation and Arrhythmic Triggers,” *Circ. Arrhythmia Electrophysiol.*, vol. 11, no. 7, pp. 1–15, 2018, doi: 10.1161/CIRCEP.117.006035.

[4] Y. Rudy and J. R. Silva, “Computational biology in the study of cardiac ion channels and cell electrophysiology,” *Q. Rev. Biophys.*, vol. 39, no. 1, pp. 57–116, 2006, doi: 10.1017/S0033583506004227.

[5] C. Carter and M. Shah, “Long QT syndrome: A therapeutic challenge,” *Ann. Pediatr. Cardiol.*, vol. 1, no. 1, p. 18, 2008, doi: 10.4103/0974-2069.41051.

 ISBN: 978-1-61208-898-3

[6] M. Deo *et al.*, "Relative contribution of changes in sodium current versus intercellular coupling on reentry initiation in 2-dimensional preparations of plakophilin-2deficient cardiac cells," *Hear. Rhythm*, vol. 8, no. 11, pp. 1740–1748, 2011, doi: 10.1016/j.hrthm.2011.06.029.

[7] M. Deo *et al.*, "KCNJ2 mutation in short QT syndrome 3 results in atrial fibrillation and ventricular proarrhythmia," *Proc. Natl. Acad. Sci. U. S. A.*, vol. 110, no. 11, pp. 4291–4296, 2013, doi: 10.1073/pnas.1218154110.

[8] L. Hou *et al.*, "A major role for hERG in determining frequency of reentry in neonatal rat ventricular myocyte monolayer," *Circ. Res.*, vol. 107, no. 12, pp. 1503–1511, 2010, doi: 10.1161/CIRCRESAHA.110.232470.

[9] M. Deo, P. Boyle, G. Plank, and E. Vigmond, "Arrhythmogenic mechanisms of the Purkinje system during electric shocks: A modeling study," *Hear. Rhythm*, vol. 6, no. 12, pp. 1782–1789, 2009, doi: 10.1016/j.hrthm.2009.08.023.

[10] M. Deo, P. M. Boyle, A. M. Kim, and E. J. Vigmond, "Arrhythmogenesis by single ectopic beats originating in the Purkinje system," *Am. J. Physiol. - Hear. Circ. Physiol.*, vol. 299, no. 4, pp. H1002–H1011, 2010, doi: 10.1152/ajpheart.01237.2009.

[11] V. Iyer, K. J. Sampson, and R. S. Kass, "Modeling tissue- and mutation- specific electrophysiological effects in the long QT syndrome: Role of the Purkinje fiber," *PLoS One*, vol. 9, no. 6, p. e97720, 2014, doi: 10.1371/journal.pone.0097720.

[12] G. Seemann, D. L. Weiß, F. B. Sachse, and O. Dössel, "Simulation of the long-QT syndrome in a model of human myocardium," *Comput. Cardiol.*, vol. 30, pp. 287–290, 2003, doi: 10.1109/cic.2003.1291147.

[13] I. Itzhaki *et al.*, "Modelling the long QT syndrome with induced pluripotent stem cells," *Nature*, vol. 471, no. 7337, pp. 225–230, 2011, doi: 10.1038/nature09747.

[14] A. D. Akwaboah *et al.*, "An in silico hiPSC-Derived Cardiomyocyte Model Built With Genetic Algorithm," *Front. Physiol.*, vol. 12, pp. 1–24, 2021, doi: 10.3389/fphys.2021.675867.

[15] G. Salama and B. London, "Mouse models of long QT syndrome," *J. Physiol.*, vol. 578, no. 1, pp. 43–53, 2007, doi: 10.1113/jphysiol.2006.118745.

[16] D. Fedida and L. Macdonald, "hERG long QT syndrome type 2 mutants need more than a chaperone to dance," *J. Physiol.*, vol. 594, no. 15, pp. 4095–4096, 2016, doi: 10.1113/JP272417.

[17] A. Mahajan *et al.*, "A rabbit ventricular action potential model replicating cardiac dynamics at rapid heart rates," *Biophys. J.*, vol. 94, no. 2, pp. 392–410, 2008, doi: 10.1529/biophysj.106.98160.

[18] O. V. Aslanidi, R. N. Sleiman, M. R. Boyett, J. C. Hancox, and H. Zhang, "Ionic mechanisms for electrical heterogeneity between rabbit purkinje fiber and ventricular cells," *Biophys. J.*, vol. 98, no. 11, pp. 2420–2431, 2010, doi: 10.1016/j.bpj.2010.02.033.

[19] F. J. Vetter and A. D. McCulloch, "Three-dimensional analysis of regional cardiac function: A model of rabbit ventricular anatomy," *Prog. Biophys. Mol. Biol.*, vol. 69, no. 2–3, pp. 157–183, 1998, doi: 10.1016/S0079-6107(98)00006-6.

[20] P. M. Boyle, M. Deo, G. Plank, and E. J. Vigmond, "Purkinje-mediated effects in the response of quiescent ventricles to defibrillation shocks," *Ann. Biomed. Eng.*, vol. 38, no. 2, pp. 456–468, 2010, doi: 10.1007/s10439-009-9829-4.

[21] A. Prassl *et al.*, "- User's Manual - Anton Prassl," 2020.

[22] D. J. Huelsing, K. W. Spitzer, J. M. Cordeiro, and A. E. Pollard, "Conduction between isolated rabbit Purkinje and ventricular myocytes coupled by a variable resistance," *Am. J. Physiol. - Hear. Circ. Physiol.*, vol. 274, no. 4 43-4, pp. 1163–1173, 1998, doi: 10.1152/ajpheart.1998.274.4.h1163.

[23] I. Schafferhofer-Steltzer, E. Hofer, D. J. Huelsing, S. P. Bishop, and A. E. Pollard, "Contributions of Purkinje-myocardial coupling to suppression and facilitation of early afterdepolarization-induced triggered activity," *IEEE Trans. Biomed. Eng.*, vol. 52, no. 9, pp. 1522–1531, 2005, doi: 10.1109/TBME.2005.851528.

[24] L. Carlsson, C. Abrahamsson, L. Drews, and G. Duker, "Antiarrhythmic effects of potassium channel openers in rhythm abnormalities related to delayed repolarization," *Circulation*, vol. 85, no. 4, pp. 1491–1500, 1992, doi: 10.1161/01.CIR.85.4.1491.

[25] C. E. Clancy and Y. Rudy, "Cellular consequences of HERG mutations in the long QT syndrome: Precursors to sudden cardiac death," *Cardiovasc. Res.*, vol. 50, no. 2, pp. 301–313, 2001, doi: 10.1016/S0008-6363(00)00293-5.

[26] K. E. Odening *et al.*, "Electrophysiological studies of transgenic long QT type 1 and type 2 rabbits reveal genotype-specific differences in ventricular refractoriness and His conduction," *Am. J. Physiol. - Hear. Circ. Physiol.*, vol. 299, no. 3, pp. H643–H655, 2010, doi: 10.1152/ajpheart.00074.2010.

[27] R. Dumaine and J. M. Cordeiro, "Comparison of K+ currents in cardiac Purkinje cells isolated from rabbit and dog," *J. Mol. Cell. Cardiol.*, vol. 42, no. 2, pp. 378–389, 2007, doi: 10.1016/j.yjmcc.2006.10.019.

[28] E. J. Vigmond, R. Weber dos Santos, A. J. Prassl, M. Deo, and G. Plank, "Solvers for the cardiac bidomain equations," Prog. Biophys. Mol. Biol., vol. 96, no. 1–3, pp. 3–18, 2008, doi: 10.1016/j.pbiomolbio.2007.07.012.

 ISBN: 978-1-61208-898-3